

## Electronic Supplementary Information

### **Earth-abundant Trigonal $\text{BaCu}_2\text{Sn}(\text{Se}_x\text{S}_{1-x})_4$ ( $x = 0 \sim 0.55$ ) Thin Films with Tunable Band Gaps for Solar Water Splitting**

*Jie Ge<sup>†</sup>, Yue Yu, and Yanfa Yan<sup>†</sup>*

Department of Physics and Astronomy & Wright Center for Photovoltaics Innovation and Commercialization, the University of Toledo, Toledo, Ohio, 43606, United States.

<sup>†</sup> Email: Jie.Ge@UToledo.Edu (Dr Jie Ge); Yanfa.Yan@UToledo.Edu (Prof Yanfa Yan)

## Experimental

### Synthesis

The precursor films were co-sputtered on the commercialized FTO glass (TEC 15, NSG) and sodium lime glass (SLG) substrates from Cu, SnS and BaS targets (Plasma Materials Co.) using the LAB Line SPUTTER 5 system (Kurt J Lesker Co.). The substrate temperature during deposition was kept relatively low (~150 °C). The Cu poor composition of precursors was precisely controlled by optimizing the radio-frequency powers for the individual targets (Cu: 42W; SnS: 45 W; BaS: 110 W). The precursors were then annealed at 540-570 °C temperatures for 30 min in a closed graphite box using sulfur or selenium powders or their mixtures, yielding the BCTSSe [BaCu<sub>2</sub>Sn(Se<sub>x</sub>S<sub>1-x</sub>)<sub>4</sub>] films with different Se/S ratios. The annealing conditions are summarized in **Table S1**.

The FTO/BCTSSe photocathodes were platinized in 0.1 M sodium sulfate solution containing 1 mM chloroplatinic acid, and the deposition was performed with a constant potential of -0.35 V vs Ag/AgCl (1 M KCl) for 2 min. During the deposition, the working electrodes were illuminated by a 30 W halogen lamp.

**Table S1** Annealing conditions for trigonal BaCu<sub>2</sub>Sn(S<sub>1-x</sub>Se<sub>x</sub>)<sub>4</sub> thin film solid solutions grown on FTO and SLG substrates.

Sample	Temperature	Sulfur powder	Selenium powder	$x = \frac{Se}{Se + S}$
FTO-1	540 °C	0.5 g	0	0
FTO-2	540 °C	0.3 g	0.2 g	0.151
FTO-3	540 °C	0.2 g	0.3 g	0.251
FTO-4	550 °C	0	0.5 g	0.510
FTO-5	560 °C	0	0.5 g	0.530
SLG-1	540 °C	0.5 g	0	0
SLG-2	540 °C	0.2 g	0.3 g	0.276
SLG-3	540 °C	0.1 g	0.4 g	0.452
SLG-4	550 °C	0	0.5 g	0.534
SLG-5	570 °C	0	0.5 g	0.555

### Characterization

X-ray diffraction (XRD) data were collected using a Rigaku Ultima III diffractometer with Cu K $\alpha$  lines (0.15418 nm) in  $\theta$ - $2\theta$  scans operated at 40 kV and 44 mA, and theta calibration was done using a standard Si sample prior to the measurement. The phase identification and the calculation of lattice constants are completed by the software of MDI Jade 2010 equipped with a monthly synchronized ICDD database (International Centre for Diffraction Data). Confocal Raman Spectroscopy was carried out using a 632.8 nm laser (HORIBA Scientific), and Raman shift was calibrated by the single crystal Si at 520.4 cm<sup>-1</sup>. The optical transmittance and reflectance of the samples were conducted with a UV-vis-NIR spectrophotometer (PerkinElmer Lambda 1050). Film compositional results and morphological images were acquired by the energy dispersive X-ray spectroscopy (EDX, Oxford) equipped with a Dual Beam Environmental hot field-emission Scanning Electron Microscope (SEM) and Focused Ion Beam system (FEI Quanta 3D FEG).

### Testing

Prior to the photoelectrochemical (PEC) measurements, the FTO/BCTSSe/Pt photocathodes were processed by chloroplatinic solution, then prepared using epoxy to cover the sample edges. The effective area of the photocathodes was determined by the software ImageJ from their digital photos. PEC measurements were carried out using a standard 3-electrode cell using a Ag/AgCl (1 M KCl) reference electrode and a platinum wire counter electrode. The linear sweep voltammetric (LSV) curves were recorded using a 300 W Xe lamp. A scan rate of 10 mV s<sup>-1</sup> in the cathodic direction was used to acquire the data. The irradiation intensity was calibrated using a standard Si cell (~100 mW cm<sup>-2</sup>). To determine the band positions of BCTSSe thin film solid solutions, we performed the dark capacitance-voltage (C-V) measurement at 10 kHz. A neutral electrolyte solution of sodium sulfite (0.5 M) and potassium phosphate (0.5 M) was used for all the PEC & IPCE & C-V measurements. A photoelectrochemistry workstation equipped with a frequency analyzer (ModuLab, Solartron Analytical) was used for all these measurements. The pH value of the electrolyte was determined to be 6.4 using a calibrated pH meter (Fisher Scientific Co.).

Potentials versus the Ag/AgCl (1 M KCl) electrode ( $E_{Ag/AgCl}$ ) were converted to reversible hydrogen electrode (RHE,  $E_{RHE}$ ) using the Nernst equation, namely,  $E_{RHE} = E_{Ag/AgCl} + 0.059 \times pH + 0.222$ . IPCE derived photocurrent densities ( $J$ ) can be integrated from the expression of  $J = \frac{e}{hc} \int \lambda(IPCE * AM1.5G)d\lambda$ .

As shown in **Fig. S6**, the linear part of Mott–Schottky (MS) plot can yield the flat band potential ( $E_{FB}$ ) of the semiconductor. The carrier density,  $N_A$ , can be calculated from the slopes of MS plot by **Eq. S1**. Furthermore, these values can be used to calculate the difference between the valence band edge ( $E_{VB}$ ) and the Fermi level ( $E_F$ ) using **Eq. S2**:<sup>1,2</sup>

$$\frac{A^2}{C^2} = \frac{2}{e\epsilon_r\epsilon_0N_A} \left( V - E_{FB} - \frac{kT}{e} \right) \quad \text{Eq. S1}$$

$$E_{VB} = -E_{FB} + kT \ln \frac{N_A}{N_V} \quad [N_V = 2 \left( \frac{2\pi m^* kT}{h^2} \right)^{\frac{3}{2}}] \quad \text{Eq. S2}$$

, where A is the area of electrode,  $e$  is element electron charge,  $\epsilon_0$  is the vacuum dielectric constant,  $\epsilon_r \approx 5.5 \sim 6.0$  (5.5 for FTO-1, 5.6 for FTO-2, 5.7 for FTO-3, 6 for FTO-4) is the relative dielectric constant of BCTSSe alloy,  $kT = 0.0259$  eV at room temperature and the effective density of states in the valence band  $N_V \approx 10^{19} \text{ cm}^{-3}$ .

**Table S2** Element atomic percentages of trigonal  $\text{BaCu}_2\text{Sn}(\text{S}_{1-x}\text{Se}_x)_4$  thin film solid solutions grown on FTO and SLG substrates, with the corresponding EDX spectra shown in Fig. S1 and Fig. S2.

Sample	Cu%	Ba%	Sn% <sup>a</sup>	S%	Se%	
FTO-1	22.18	12.64	13.13	52.06	0	
FTO-2	19.60	10.04	24.31	39.11	6.94	
FTO-3	17.62	10.43	25.70	34.64	11.61	
FTO-4	18.63	10.33	23.84	23.15	24.05	
FTO-5	Spectrum 1	18.93	10.40	21.68	22.89	26.11
	Spectrum 2	19.06	8.40	22.72	18.63	31.19
	Spectrum 3	18.30	10.35	25.83	22.87	25.83
	Spectrum 4	19.20	9.09	23.16	23.59	24.96
SLG-1	22.95	13.17	13.05	50.84	0	
SLG-2	Spectrum 1	23.48	12.99	11.45	39.93	12.15
	Spectrum 2	22.71	13.21	13.04	36.96	14.09
SLG-3	Spectrum 1	23.70	13.47	13.11	27.23	22.49
	Spectrum 2	19.35	11.54	11.96	32.59	24.56
SLG-4	23.87	12.56	12.55	23.55	27.47	
SLG-5	25.17	13.60	12.72	21.20	26.50	

<sup>a</sup> Sn percentages from films based on FTO substrates are not real, since FTO substrates contribute additional EDX signals

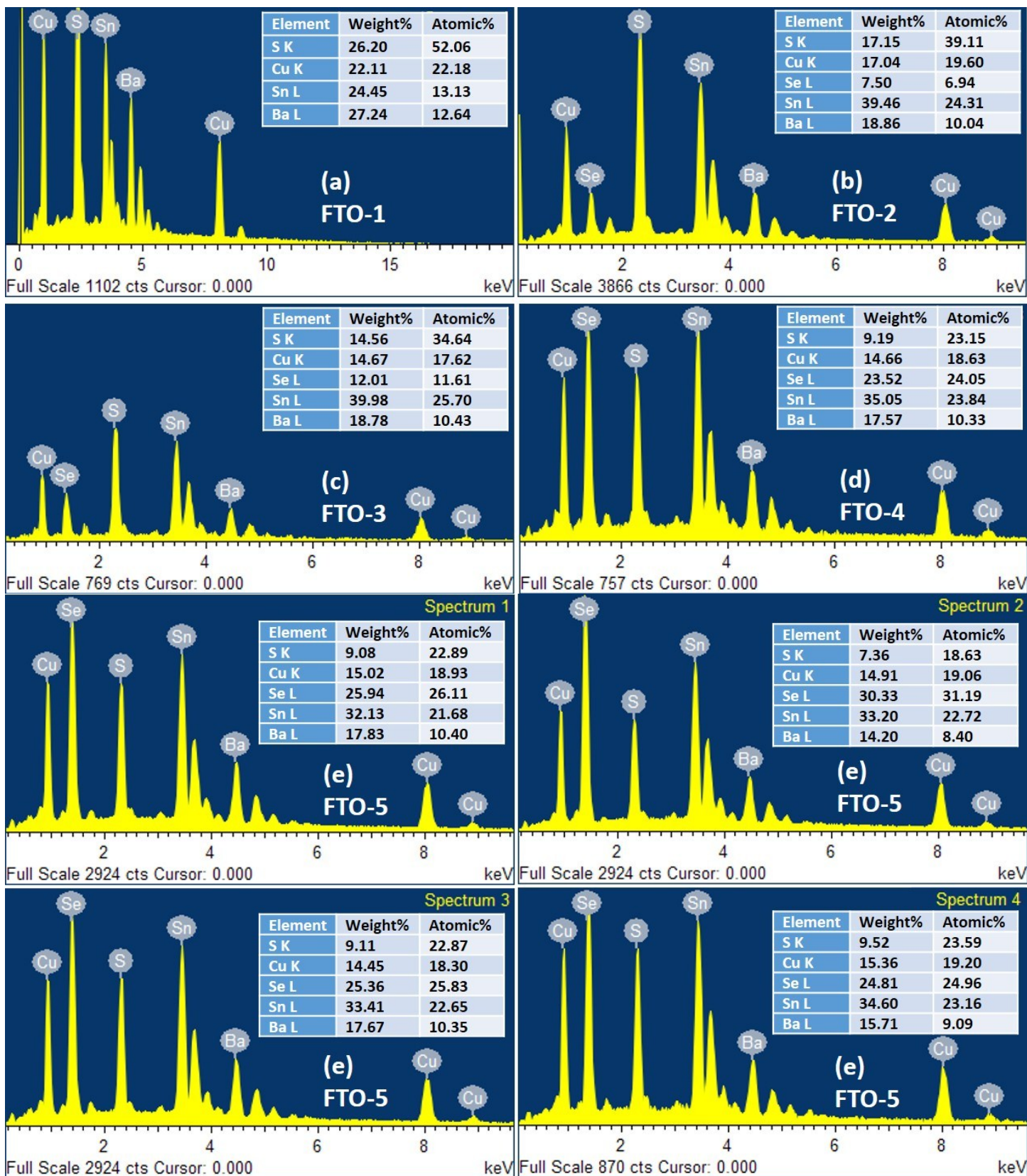


**Fig. S1** EDX spectra of trigonal  $\text{BaCu}_2\text{Sn}(\text{S}_{1-x}\text{Se}_x)_4$  thin film solid solutions grown on FTO substrates with different compositions  $x=\text{Se}/(\text{Se}+\text{S})$ .

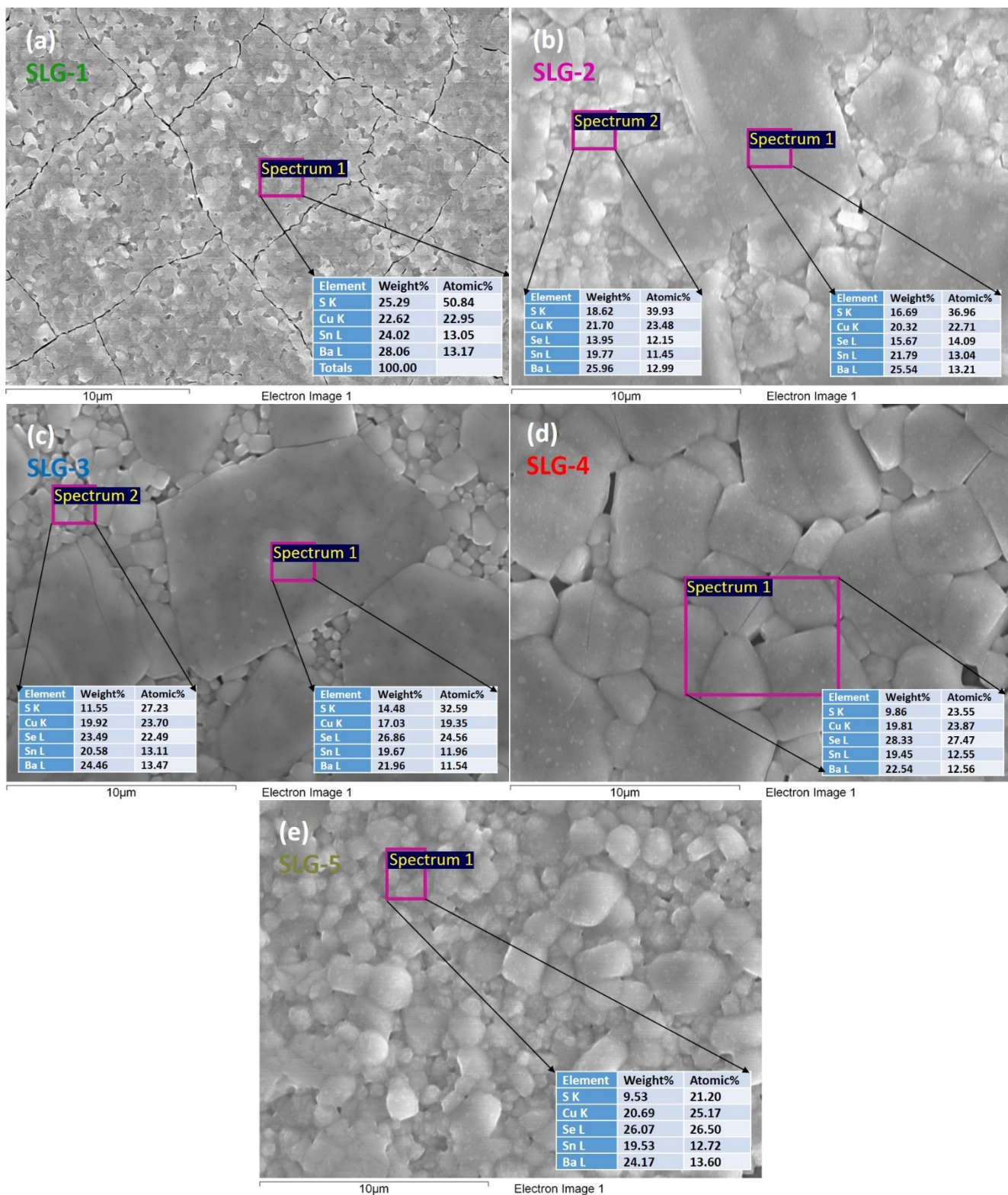


**Fig. S2** SEM morphological images of trigonal  $\text{BaCu}_2\text{Sn}(\text{S}_{1-x}\text{Se}_x)_4$  thin film solid solutions grown on SLG substrates with different compositions  $x=\text{Se}/(\text{Se}+\text{S})$ . The compositional results were acquired from the boxed areas by EDX spectra. Note: BCTSSe films show the non-ideal morphologies including “cracks” in Panel a, “non-uniform grains and compositions” in Panel b and Panel c, possibly due to annealing at high temperatures exceeding the softening point of SLG substrates.

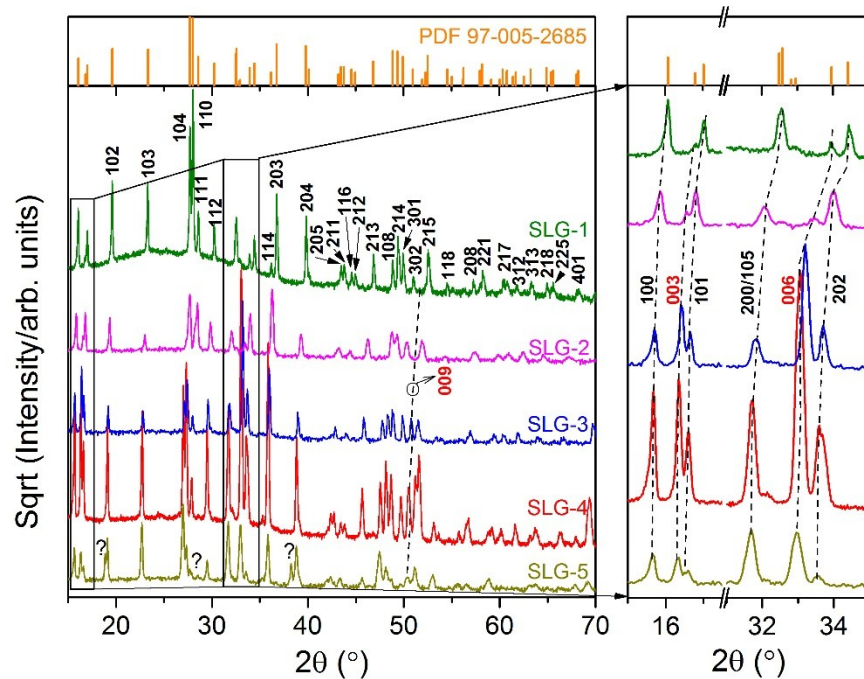


**Fig. S3** X-ray diffraction (XRD) patterns of trigonal  $\text{BaCu}_2\text{Sn}(\text{S}_{1-x}\text{Se}_x)_4$  thin film solid solutions grown on SLG substrates (a), with the magnified patterns from the regions of interest showing the variances in lattice constant and growth orientation; Note: the peaks labeled with “?” at  $18.874^\circ$ ,  $28.529^\circ$  and  $38.257^\circ$  correspond to  $\text{CuSe}_x$  secondary phases (PDF #00-18-0453 & 00-47-1745); the remaining peaks are indexed to trigonal  $\text{BaCu}_2\text{SnS}_4$  (red markers in the top panels, PDF 97-005-2685).

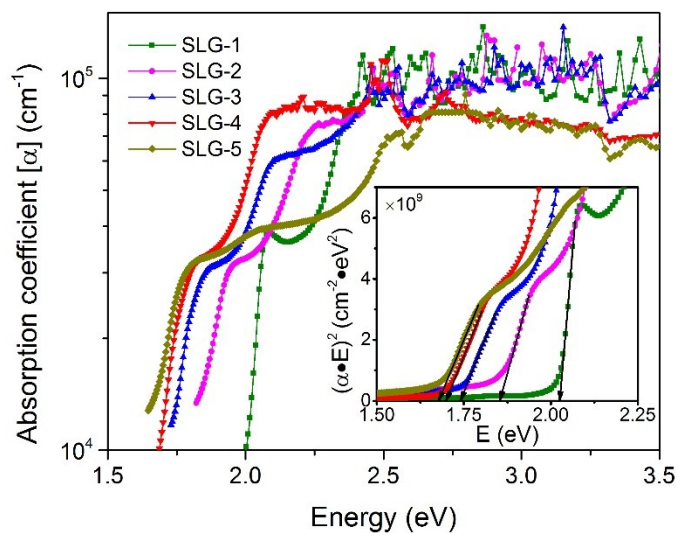


**Fig. S4** Optical absorption coefficients  $[\alpha]$  of and trigonal  $\text{BaCu}_2\text{Sn}(\text{S}_{1-x}\text{Se}_x)_4$  thin film solid solutions grown on SLG glass substrates, with band gap estimation based on Tauc plot of  $(\alpha \cdot E)^2 \propto E$  in the insets.

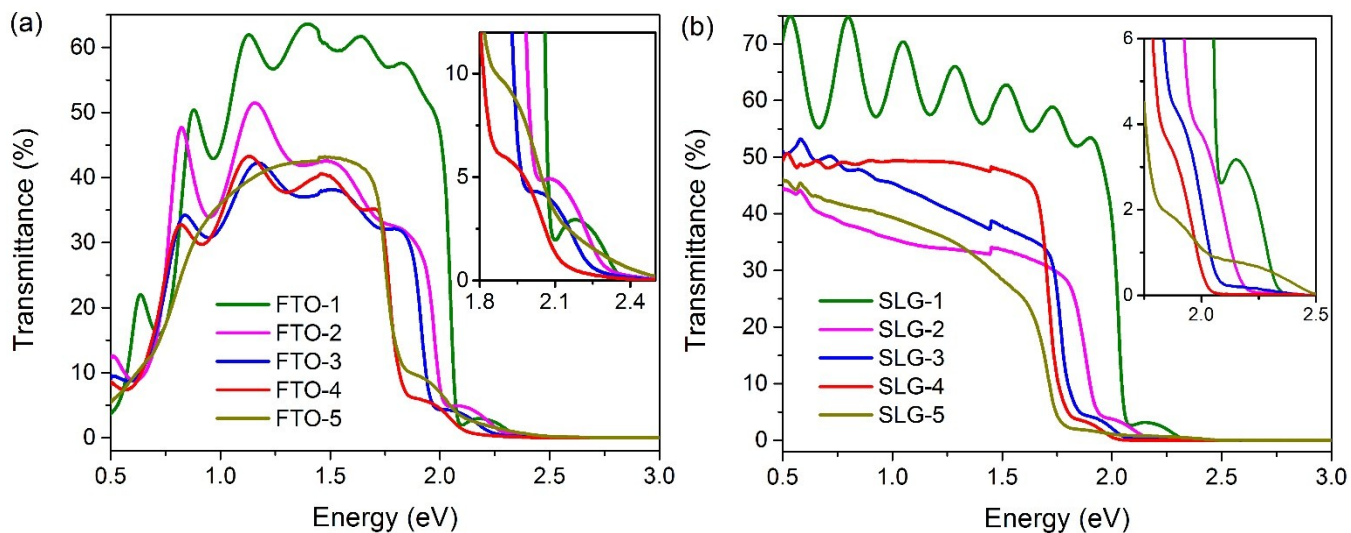


**Fig. S5** Optical transmission spectra of trigonal  $\text{BaCu}_2\text{Sn}(\text{S}_{1-x}\text{Se}_x)_4$  thin films grown on FTO (a) and SLG (b) substrates, with the insets showing the magnified spectra ranging from 1.75 eV to 2.5 eV.

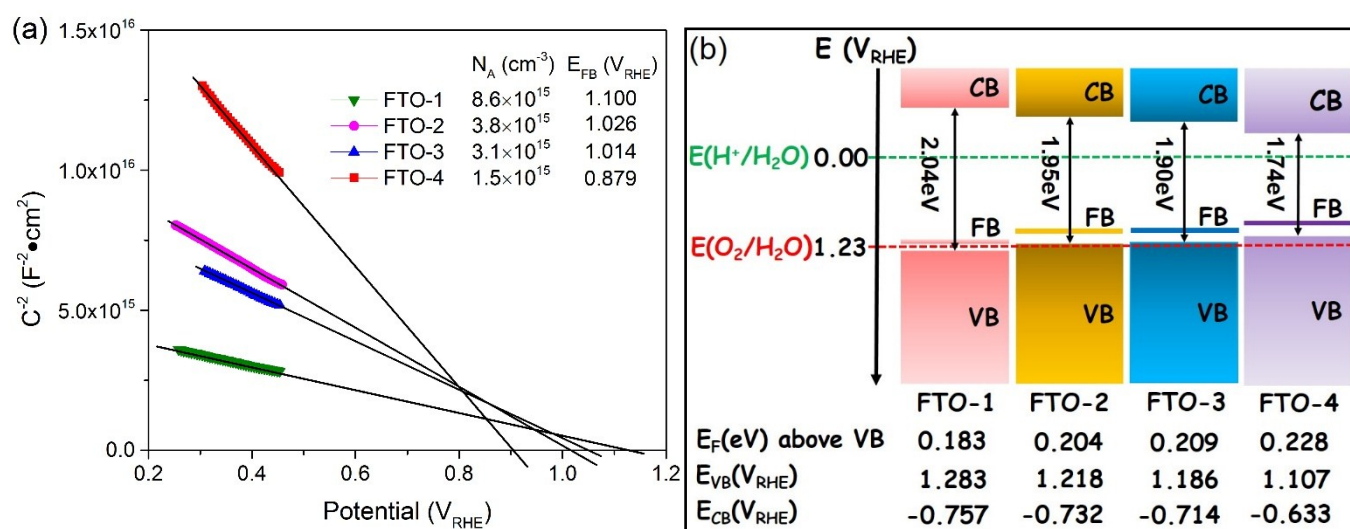


**Fig. S6** Capacitance-voltage (C-V) derived Mott-Schottky (MS) plots of FTO/BCTSSe electrodes measured in dark at 10 kHz using 3-electrode configuration in a neutral electrolyte (a); MS-derived band position diagrams of BCTSSe thin film solid solutions with respect to hydrogen evolution potential  $E(\text{H}^+/\text{H}_2\text{O})$  and oxygen evolution potential  $E(\text{O}_2/\text{H}_2\text{O})$  (b). CB—conduction band, VB—valence band, FB—flat band,  $E_{\text{F}}$ —Fermi level, RHE—reversible hydrogen electrode.



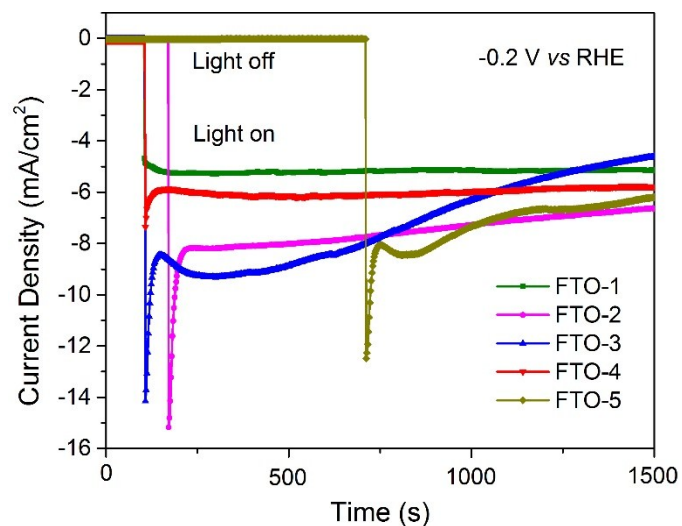


**Fig. S7** Chronoamperometric curves showing the stability of photocurrent at  $-0.2\text{ V vs RHE}$ . The electrodes were processed with a  $1\text{ mM}$  chloroplatinic solution prior to PEC testing. All the measurements were carried out using a 3-electrode configuration in a neutral electrolyte ( $\text{pH} = 6.4$ ).

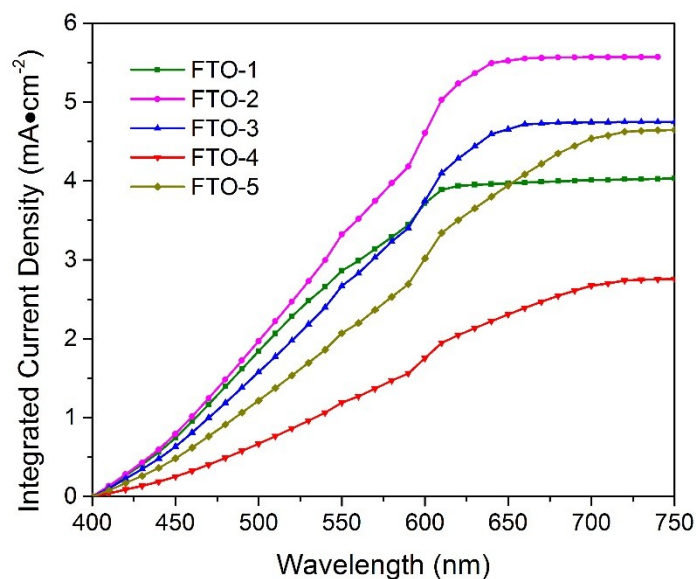


**Fig. S8** Integrated current density from the IPCE data shown in Fig. 5b.

#### Additional Reference

1. X. Shi, L. Cai, M. Ma, X. Zheng and J. H. Park, *ChemSusChem*, 2015, **8**, 3192-3203.
2. J. A. Turner, *Journal of Chemical Education*, 1983, **60**, 327.